Expression of a TMC6-TMC8-CIB1 heterotrimeric complex in lymphocytes is regulated by each of the components

Received for publication, February 14, 2020, and in revised form, September 9, 2020 Published, Papers in Press, September 11, 2020, DOI 10.1074/jbc.RA120.013045

Chuan-Jin Wu[1,‡], Xing Li[2,‡], Connie L. Sommers[1,‡], Kiyoto Kurima[2], Sunmee Huh[1], Grace Bugos[1], Lijin Dong[3], Wenmei Li[1], Andrew J. Griffith[2], and Lawrence E. Samelson[1,*]

From the [1]Laboratory of Cellular and Molecular Biology, Center for Cancer Research, National Cancer Institute, Bethesda, Maryland, USA, the [2]Molecular Biology and Genetics Section, National Institute on Deafness and Other Communication Disorders, National Institutes of Health, Rockville, Maryland, USA, and the [3]Genetic Engineering Core, National Eye Institute, National Institutes of Health, Bethesda, Maryland, USA

Edited by Craig E. Cameron

The *TMC* genes encode a set of homologous transmembrane proteins whose functions are not well understood. Biallelic mutations in either *TMC6* or *TMC8* are detected in more than half of cases of the pre-malignant skin disease epidermodysplasia verruciformis (EV). It is controversial whether EV induced by mutations in TMC6 or TMC8 originates from keratinocyte or lymphocyte defects. Quantification of TMC6 and TMC8 RNA levels in various organs revealed that lymphoid tissues have the highest levels of expression of both genes, and custom antibodies confirmed protein expression in mouse lymphocytes. To study the function of these proteins we generated mice with targeted deletion mutant alleles of *Tmc6* or *Tmc8*. Either TMC6 or TMC8 deficiency induced a reduction in apparent molecular weight and/or amount of the other TMC molecule. Co-immunoprecipitation experiments indicated that TMC6 and TMC8 formed a protein complex in mouse and human T cells. MS and biochemical analysis demonstrated that TMC6 and TMC8 additionally interacted with the CIB1 protein to form TMC6-TMC8-CIB1 trimers. We demonstrated that TMC6 and TMC8 regulated CIB1 levels by protecting CIB1 from ubiquitination and proteasomal degradation. Reciprocally, CIB1 was needed for stabilizing TMC6 and TMC8 levels. These results suggest why inactivating mutations in any of the three human genes leads to similar clinical presentations. We also demonstrated that TMC6 and TMC8 levels are drastically lower and the proteins are less active in regulating CIB1 in keratinocytes than in T cells. Our study suggests that defects in lymphocytes may contribute to the etiology and pathogenesis of EV.

The discovery that mutations in the *TMC1* and *Tmc1* genes caused deafness in humans and mouse models, respectively, led to basic insights into the mechanism of hearing (1). *Tmc1* is expressed in sensory hair cells of the cochlea and vestibular organs of the inner ear. A series of studies has demonstrated that TMC1 is a polytopic transmembrane protein that contributes to the pore of the long-sought mechanoelectrical transduction channel at the tips of inner ear hair cell stereocilia bundles (2–8).

Following identification of *TMC1*, bioinformatic and genetic analysis revealed seven more human paralogs and mouse sequences with high sequence conservation (1). Two other *TMC* genes, *TMC6* and *TMC8*, were shown to be the previously described *EVER1* and *EVER2* genes which, when mutated, cause epidermodysplasia verruciformis (EV) (9). Patients with this disease are susceptible to human papillomavirus (HPV) infections that cause skin lesions that can progress to squamous cell carcinoma. Considered an immunodeficiency disease, it has been controversial whether immune cells, keratinocytes, or both are the primarily affected cell type in EV (10, 11).

The anoctamin family of transmembrane proteins contains 10 members. Evidence for channel and lipid flippase activities of the anoctamins has been presented (12). As with the TMC family, mutations in several anoctamin genes lead to various diseases, and overexpression of some of the anoctamins are implicated in cancer development. Biochemical experiments showed that the anoctamin proteins are expressed as dimers, and structural studies confirmed this topology (13, 14). Of further relevance to our studies is that bioinformatic analysis suggested that the anoctamin and TMC families of proteins are evolutionarily related because they demonstrate sequence similarity and were predicted to have similar membrane topology (15).

Patients with EV without mutations in *TMC6* or *TMC8* but with null mutations of the *CIB1* (calcium- and integrin-binding protein 1) gene have recently been described (16). The authors suggested that the absence of CIB1 in keratinocytes contributed to the disease in these patients. CIB1 was proposed in this study to be found in complex with TMC6 and TMC8 proteins. Evidence for this hypothesis was indirect because manipulation of TMC6 and TMC8 mRNA levels could affect CIB1 protein levels, and incomplete because only CIB1 proteins could be directly detected.

To further define the role of *TMC6* and *TMC8* in T cell function and in models of EV, we analyzed expression of these genes in murine tissues and generated mice segregating targeted deletion alleles of *Tmc6* and *Tmc8*. To enable studies of the TMC6 and TMC8 proteins, we also generated specific antibodies for both of these proteins. We found that both genes were highly expressed in murine T cells. At the protein level, we demonstrated that TMC6 and TMC8 heterodimerize and confirmed that they form a trimeric complex with CIB1. Levels of both TMC proteins and CIB1 cross-regulate each other. Finally, we

This article contains supporting information.
‡These authors contributed equally to this work.
*For correspondence: Lawrence E. Samelson, samelsonl@helix.nih.gov.

Published in the U.S.A.

found that TMC6 is expressed more than 6.6-fold higher in T cells than in keratinocytes and that expression of TMC8 is very low in keratinocytes. Our data define the existence of a complex containing TMC6-TMC8-CIB1 and provide further basic information relevant to the study of EV.

Results

Although *TMC6* and *TMC8* mutations have been linked to abnormal susceptibility to β-HPV infection and the disease epidermodysplasia verruciformis, little is known about the physiological functions of the channel-like proteins encoded by these genes. To study TMC6 and TMC8 biological functions and to provide a mouse model to investigate EV, we generated mice in which loss-of-function mutations of *Tmc6* or *Tmc8* alleles ($Tmc6^{\Delta}$ or $Tmc8^{\Delta}$, respectively) were generated by recombination-introduced deletions. The molecular strategy was analogous to that used to generate functional null alleles of *Tmc1* and *Tmc2* (4) (Fig. 1, *A* and *B*). Southern blotting analysis verified the deletions of relevant *Tmc6* or *Tmc8* genomic DNA fragments (Fig. 1, *A* and *B*). We examined *Tmc6* and *Tmc8* RNA expression in various mouse organs by Northern blotting analysis and observed that *Tmc6* and *Tmc8* RNA levels were highest in thymus, lung, and spleen among the examined tissues (Fig. 1*C*). These results are consistent with *TMC6* and *TMC8* RNA data for human organs, which show that lymphoid tissues such as lymph node and spleen express *TMC6* and *TMC8* RNA at much higher levels than a variety of other tissues (protein atlas HPA data set, RRID:SCR_006710).

Because we found no reliable commercial antibodies specific for TMC6 or TMC8, we analyzed the published protein sequences of these proteins to inform the design of specific immunogens. We observed protein-specific amino acid sequences in their predicted cytosolic carboxyl termini. We generated and expressed chimeric fusion proteins of each of the TMC6- and TMC8-specific C-terminal regions with glutathione S-transferase (GST) (Fig. S1) and used the purified proteins to immunize rabbits. Affinity-purified polyclonal anti-TMC6 and a monoclonal anti-TMC8 were capable of specifically detecting the corresponding TMC proteins in mouse thymocytes by Western blotting. Distinct bands corresponding to TMC6 or TMC8 were seen in lysates from WT thymocytes, whereas the corresponding TMC6 or TMC8 signals were completely missing from $Tmc6^{\Delta/\Delta}$ or $Tmc8^{\Delta/\Delta}$ thymocytes (Fig. 1*D*). Notably, we consistently observed that the relative mobility of the TMC6 band increased (*i.e.* the molecular weight presumably decreased) and the TMC6 band intensity levels were decreased in $Tmc8^{\Delta/\Delta}$ mice. TMC8 protein was detected as a doublet in WT thymocytes; however, the upper band of this doublet was absent in $Tmc6^{\Delta/\Delta}$ thymocytes (Fig. 1*D* and Fig. S2). All of these changes appeared to occur at the protein level, because qRT-PCR analysis found neither *Tmc8* mRNA reduction in $Tmc6^{\Delta/\Delta}$ thymocytes nor *Tmc6* mRNA reduction in $Tmc8^{\Delta/\Delta}$ thymocytes (Fig. 1*E*) We also observed high TMC6 and TMC8 protein expression in peripheral lymphocytes. CD4 T cells, CD8 T cells, and B cells all expressed high levels of TMC6 and TMC8 proteins (Fig. 1*F*).

The crystal structure of the TMC homolog anoctamin or TMEM16 family member nhTMEM16 (from the fungus *Nectria hematococca*) demonstrated that the anoctamin protein forms a homodimer (14). Given that TMC6 and TMC8 reciprocally regulate the expression levels of each other at the protein level (Fig. 1*D* and Fig. S2), we asked whether TMC6 and TMC8 interact to form a heterodimer. We performed TMC6 and TMC8 reciprocal co-immunoprecipitation assays from mouse thymocyte lysates. $Tmc6^{\Delta/\Delta}$ and $Tmc8^{\Delta/\Delta}$ controls were included to confirm that the signals detected by the antibodies were specific. Both TMC6 and TMC8 co-immunoprecipitated with the other protein. By analogy to the anoctamin structure, our results demonstrate that TMC6 and TMC8 indeed form or are components of a heterodimeric complex in mouse thymocytes, though more complex structures are not excluded (Fig. 2*A*). Furthermore, to demonstrate that human TMC6 and TMC8 can interact, we transfected human Jurkat T cells with FLAG-tagged hTMC6 and HA-tagged hTMC8 (Fig. 2*B*, transient transfection and Fig. 2*C*, stable transfection) and used specific anti-peptide tag antibodies for immunoprecipitation and immunoblotting. The transiently transfected FLAG-TMC6 and HA-TMC8 protein levels were below the detection limit of high-affinity anti-FLAG or anti-HA antibodies in cell lysate inputs (Fig. 2*B*, *lanes e–h*), suggesting that the proteins were expressed at low levels in the transiently transfected Jurkat cells (transfection efficiencies >60% were observed for a GFP plasmid transfection, data not shown). Nonetheless, the TMC proteins were both clearly seen in the immunoprecipitates brought down by the antibody against the other protein in TMC6- and TMC8-cotransfected cells (Fig. 2*B*, *lanes d and l*) but not in any cells transfected only with TMC6 or TMC8 (Fig. 2*B*, *lanes b*, *c*, *j*, *and k*). TMC6 and TMC8 proteins were not detected via Western blotting in several mouse T cell lines (data not shown), and it appears that these proteins are endogenously expressed at low levels in Jurkat cells. We then performed stable transduction or transfection of TMC6 and TMC8 into Jurkat cells and screened to acquire clones in which the tagged TMC6 and TMC8 were detectable via Western blotting for Fig. 2*C* and later experiments. Again, co-immunoprecipitation of TMC6 with TMC8 was seen in the anti-HA (TMC8) immunoprecipitates from cells stably coexpressing TMC6 and TMC8 (Fig. 2*C*).

$Tmc6^{\Delta/\Delta}$ and $Tmc8^{\Delta/\Delta}$ mice bred and grew normally. No general abnormalities were observed up to the age of 18 months. Because high TMC6 and TMC8 expression were seen in lymphocytes, including T cells, and T cells play a critical role in immune defense against various infections, we characterized T cell development in $Tmc6^{\Delta/\Delta}$ and $Tmc8^{\Delta/\Delta}$ mice. We did not detect a major defect in T cell subset numbers or function. As an alternative approach to determine the function of these proteins, we turned to using MS to identify TMC6- and TMC8-interacting proteins to gain insight into the potential molecular basis of their physiological functions. Given that TMC6 and TMC8 interact and that their expression levels reciprocally affect each other, TMC6 and TMC8 protein complex formation might be important for TMC6 and TMC8 regulation of other proteins. Thus, we used Jurkat cells that were stably transfected with both TMC6 and TMC8 to identify additional interacting proteins. TMC6 or TMC8 peptides were detected by MS in the

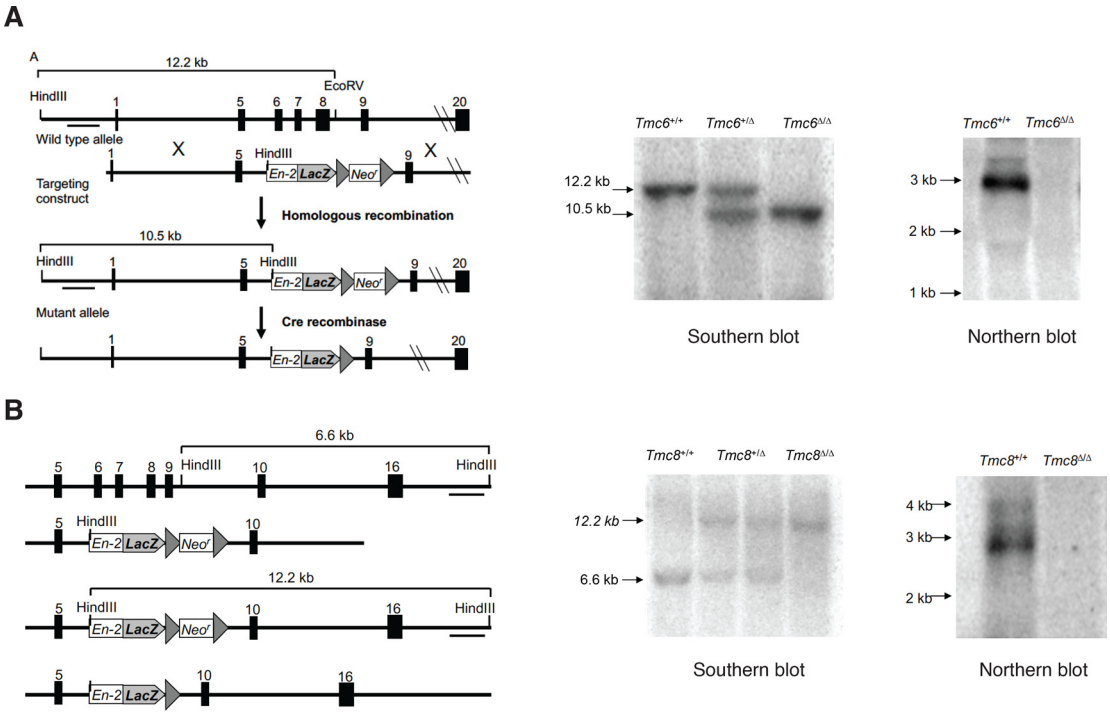
A
12.2 kb
EcoRV
HindIII
Wild type allele
Targeting construct
Homologous recombination
10.5 kb
Mutant allele
Cre recombinase
En-2 LacZ
Neo'
Southern blot
Northern blot
B
6.6 kb
12.2 kb
Southern blot
Northern blot
C
Brain(N)
Thymus(N)
Thymus(A)
Lung(N)
Lung(A)
Spleen(N)
Spleen(A)
Skin(N)
Skin(A)
Tmc6
Tmc8
D
WT 1
WT 2
kDa
TMC6
TMC8
β-Actin
E
Relative RNA amounts
F
Thymocytes
Total periphery lymphocytes
CD4 T cells
CD8 T cells
B cells

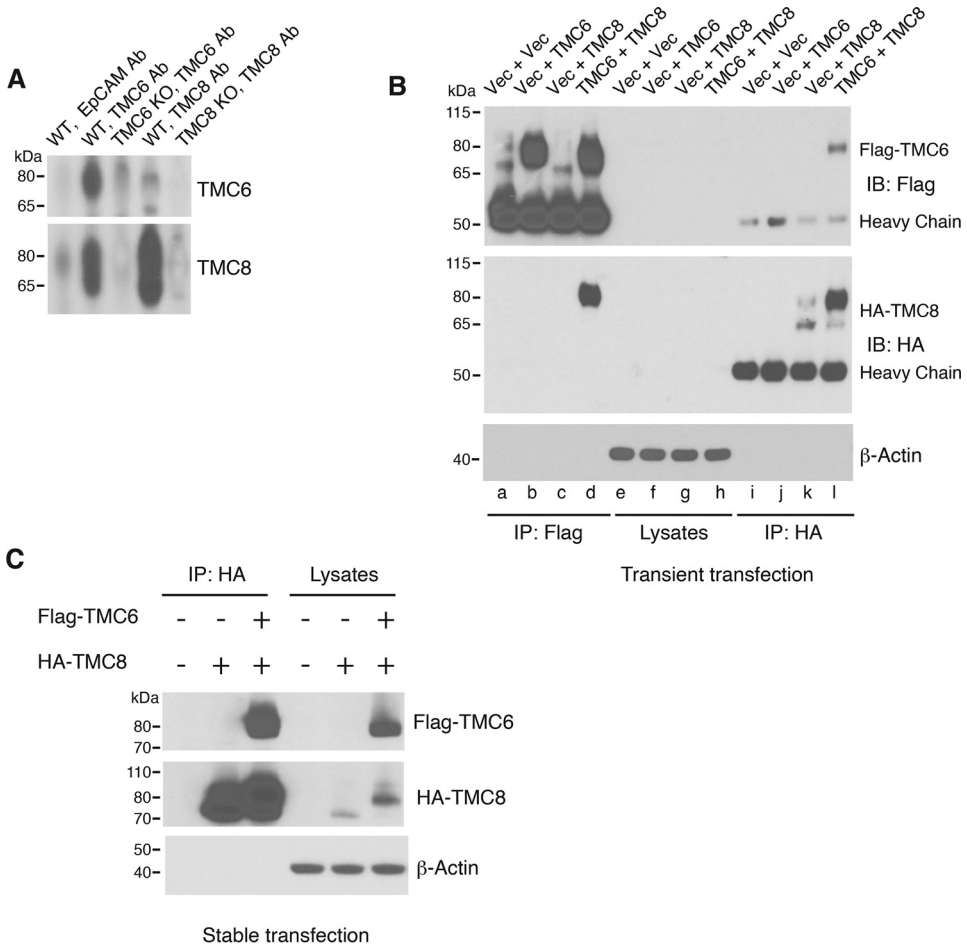

Figure 2. TMC6 and TMC8 form a complex. *A*, thymocytes from age-matched female WT, *Tmc6*$^{\Delta/\Delta}$, or *Tmc8*$^{\Delta/\Delta}$ mice were prepared and lysed in Triton X-100 buffer. Cell lysates normalized based on protein concentration were immunoprecipitated with rabbit anti-TMC6, anti-TMC8, or anti-EpCAM (control) Ab. Immunoprecipitates were subjected to SDS-PAGE separation and Western blotting detection of TMC6 and TMC8 with anti-TMC6 and anti-TMC8 Ab. *B*, combinations of empty vectors or plasmids encoding FLAG-tagged human TMC6 or HA-tagged human TMC8 were transfected into Jurkat cells using electroporation. The cells were harvested at 48 h after transfection and lysed in Triton X-100 lysis buffer. Cell lysates normalized for protein contents were immmunoprecipitated with anti-FLAG (*lanes a–d*) or anti-HA antibody (*lanes i–l*). Immunoprecipitates and cell lysate inputs (*lanes e–h*) were resolved by SDS-PAGE and immunoblotted with anti-FLAG or anti-HA to detect TMC6 or TMC8 proteins. *C*, normalized Triton cell lysates from Jurkat cells stably transfected with empty vectors, HA-TMC8 expression plasmid, or HA-TMC8 expression plasmid plus FLAG-TMC6 plasmid were immunoprecipitated with anti-HA Ab. Immunoprecipitates and lysate inputs were resolved and probed for the presence of FLAG-TMC6 or HA-TMC8 by immunoblotting with anti-FLAG or anti-HA Ab.

corresponding protein immunoprecipitates bound by anti-HA or anti-FLAG Ab. There were nearly comparable numbers of TMC6 or TMC8 peptide spectrum matches (PSMs) to the PSMs of the other host proteins detected by MS in the TMC6 or TMC8 immunoprecipitates (Fig. S3). These results again indicate a strong interaction between TMC6 and TMC8, as seen in Fig. 2. Notably, large numbers of calcium and integrin-binding protein 1 (CIB1) PSMs were also detected in both TMC6 and TMC8 immunoprecipitates from cells cotransfected with TMC6 and TMC8 but not from control cells (Fig. S3, *A* and *B*). Other abundant PSMs were not specifically co-immunoprecipitated. These results support the previous observation of CIB1 as a protein

Figure 1. Generation of targeted deletion alleles of mouse *Tmc6* and *Tmc8* and expression studies of RNA and protein encoded by these genes. *A*, strategy for homologous recombination to delete exons 6–8 and generate transcripts with premature translation termination codons. The bars under the WT and mutant alleles indicate locations of probes for Southern blotting hybridization. Elimination of the neomycin resistance gene used for selection was accomplished with Cre recombinase. The Southern blotting shows confirmation of homologous recombination. The Northern blotting depicts RNA from thymus probed with *Tmc6* probe 1. *B*, strategy for homologous recombination to delete exons 6–9 of *Tmc8* and generate transcripts encoding premature termination codons. The bars under the WT and mutant alleles indicate location of the probe for Southern blotting analysis. Elimination of the neomycin resistance gene used for selection was accomplished with Cre recombinase. The Southern blotting shows confirmation of homologous recombination. The Northern blotting depicts thymus RNA probed with *Tmc8* probe 1. *C*, northern blotting of adult (*A*, ≥10 weeks old) and neonatal (*N*, 3 days old) mouse tissues using *Tmc6* and *Tmc8* probes. *D*, Triton cell lysates of thymocytes from separate 8–10-week-old WT, *Tmc6*$^{\Delta/\Delta}$, and *Tmc8*$^{\Delta/\Delta}$ mice immunoblotted with anti-TMC6 or anti-TMC8 antibody. β-Actin was used as a loading control. *E*, total RNA was extracted from thymocytes of two 9–12-week-old WT, *Tmc6*$^{\Delta/\Delta}$, or *Tmc8*$^{\Delta/\Delta}$ mice and subjected to real-time RNA analysis of *Tmc6* and *Tmc8* mRNA levels. Sample levels are expressed relative to β-actin mRNA levels and were normalized such that expression levels in WT mouse 1 (*WT 1*) = 1. *F*, Western blotting analysis of TMC6 and TMC8 in mouse peripheral lymphocytes. Combined lymph node and spleen cells from three 8–10-week-old C57BL/6 mice were purified for CD4, CD8, or B cells. Cell purity (>88%) was verified using flow cytometry analysis after staining with anti-CD4, anti-CD8, or anti-B220 antibody. Cell lysates from nonpurified combined lymph node and spleen lymphocytes, purified lymphocytes, or combined thymocytes from the same three mice were resolved via SDS-PAGE and immunoblotted using anti-TMC6 and anti-TMC8 Ab.

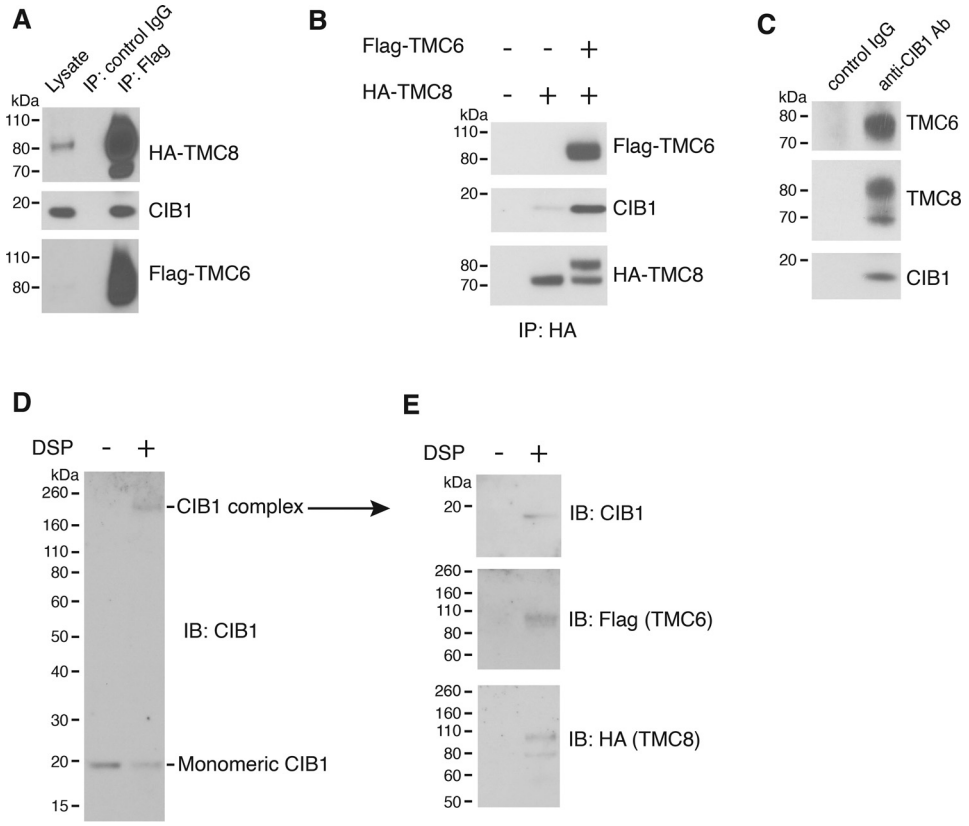

Figure 3. TMC6 and TMC8 interact with CIB1. *A*, cell lysates from Jurkat cells that stably express FLAG-TMC6 and HA-TMC8 were immunoprecipitated with anti-FLAG antibody or control IgG. The resolved immunoprecipitates were immunoblotted with anti-HA, anti-CIB1, or anti-FLAG Ab. *B*, cell lysates from Jurkat cells with stably transfected control empty vectors, HA-TMC8, or both FLAG-TMC6 and HA-TMC8 were immunoprecipitated with anti-HA Ab. The immunoprecipitates were resolved and immunoblotted with anti-FLAG, anti-CIB1, or anti-HA. *C*, thymocyte lysates from a 2-month-old mouse were immunoprecipitated with anti-CIB1 antibody or control IgG. The resulting immunoprecipitates were resolved by SDS-PAGE, and TMC6 and TMC8 were detected by immunoblotting. *D*, Jurkat cells that stably express FLAG-TMC6 and HA-TMC8 were treated with DMSO or 2 mM DSP. Cell lysates were normalized based on protein concentrations and then resolved on a 4–12% Bis-Tris NuPAGE gel under nonreducing conditions and immunoblotted with anti-CIB1 Ab. *E*, the CIB1 Ab-detected ~200-kDa band (*arrow-labeled*) in the DSP lane or the corresponding slice in the DMSO lane were cut from a replicate gel as in (*D*) and eluted in reducing sample buffer. The elutes were then separated on a second SDS-PAGE gel and immunoblotted for detection of CIB1, TMC6, and TMC8 by probing with anti-CIB1, anti-FLAG, or anti-HA Ab.

interacting with TMC6 and TMC8 in a study of overexpressed proteins in HEK293 cells (16).

We verified, using Western blotting analysis, that endogenous CIB1 indeed co-immunoprecipitated with TMC6 and TMC8 in Jurkat cells transfected to stably express these two proteins (Fig. 3*A*). Markedly more CIB1 was detected in the TMC8 immunoprecipitates in cells transfected with and expressing both TMC6 and TMC8 than in cells transfected only with TMC8, suggesting that TMC6 and TMC8 complex formation enhances the TMC8-CIB1 interaction (Fig. 3*B*). Importantly, we also demonstrated that endogenous TMC6 and TMC8 interact with endogenous CIB1 in mouse thymocytes in a similar co-immunoprecipitation study (Fig. 3*C*). These results are consistent with the idea that TMC6, TMC8, and CIB1 form a heterotrimeric protein complex in cells. To verify this possibility experimentally, we treated Jurkat cells expressing the stable FLAG-TMC6 and HA-TMC8 with or without the cleavable cross-linker dithiobis(succinimidyl propionate) (DSP). Detergent lysates from these two preparations were separated by SDS-PAGE and transferred for blotting under nonreducing conditions. In addition to the 17-kDa monomeric CIB1 band, CIB1 antibody detected another ~200-kDa band containing CIB1 only in the preparation treated with DSP (Fig. 3*D*). The ~200 kDa size is consistent with the sum of molecular weights of monomeric CIB1, TMC6, and TMC8. A similar preparation was treated identically but was not transferred. The region of this second gel containing the 200-kDa band was excised and subjected to elution in the presence of the reducing agent DTT. The eluents from noncrosslinked and crosslinked reduced proteins from the 200-kDa region were re-electrophoresed, transferred, and subjected to immunoblotting. The specifically crosslinked and subsequently reduced 200-kDa band did indeed contain monomeric CIB1, TMC6, and TMC8, thus demonstrating that these molecules form a heterotrimer (Fig. 3*E*).

In addition to interacting with CIB1, TMC6 and TMC8 coexpression robustly elevated CIB1 levels in Jurkat cells. TMC6 or TMC8 transfection alone was sufficient to elevate CIB1 levels (Fig. 4*A*, Triton buffer lysates, and Fig. 4*B*, more stringent RIPA buffer lysates). Comparison of cells transfected only with TMC6 or TMC8 to cells transfected with both, as shown in Fig. 4*B*, suggested that coexpression and thus TMC6-TMC8 complex formation may further enhance the capacity of TMC6 and TMC8 to regulate CIB1 levels. Additionally,

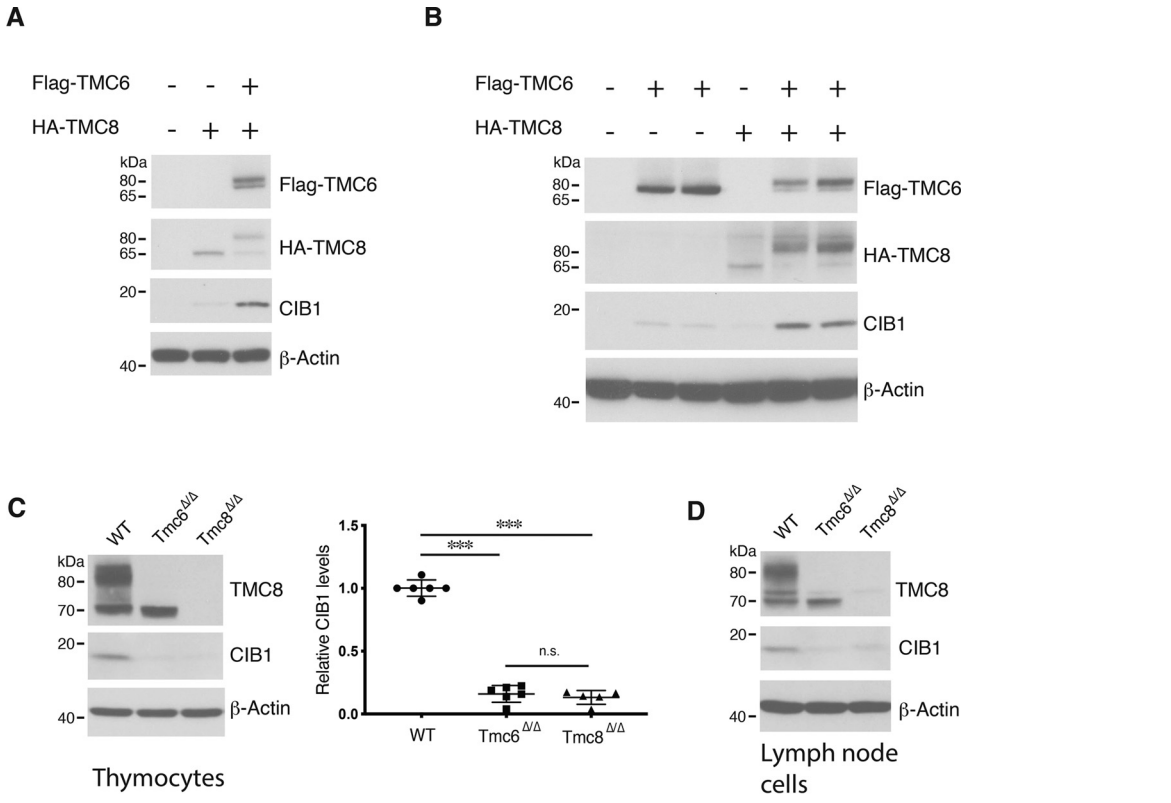

Figure 4. TMC6 and TMC8 regulate CIB1 levels in lymphocytes. *A*, Triton cell lysates from Jurkat cells that were stably transfected with control vectors, HA-TMC8, or both HA-TMC8 and FLAG-TMC6 were resolved by SDS-PAGE and immunoblotted with anti-FLAG, anti-HA, or anti-CIB1. β-Actin was used as a loading control. *B*, RIPA cell lysates prepared from Jurkat cells with stably transfected empty vectors, two clones of cells that stably express FLAG-TMC6, and stable Jurkat/HA-TMC8 cells that were stably transfected with empty vector or FLAG-TMC6 (two clones). Cell lysates were normalized based on protein concentration and tested for FLAG-TMC6, HA-TMC8, and CIB1 levels by Western blotting. Cell lysates of thymocytes (*C*) or lymph node cells (*D*) from 8–10-week-old female WT, *Tmc6*$^{\Delta/\Delta}$, or *Tmc8*$^{\Delta/\Delta}$ mice were normalized for protein concentration and immunoblotted with anti-CIB1 to determine cellular CIB1 levels. CIB1 band intensities in the experiments shown as the *left panel* in (*C*) were quantified and normalized to β-actin. Data are depicted as mean ± S.D. of the values relative to WT = 1. A one-way analysis of variance was used to assess mean differences between groups. *p* value of comparison of CIB1 expression between WT ($n = 7$) and *Tmc6*$^{\Delta/\Delta}$ ($n = 7$) or between WT ($n = 7$) and *Tmc8*$^{\Delta/\Delta}$ ($n = 6$) is <0.001(***). *n.s.*, not significant.

coexpression of TMC6 and TMC8 largely increased the detectable fraction of the larger species of the other protein. Coexpression of TMC6 also elevated TMC8 band intensities (Fig. 4*B*). These results from our analysis of transfected human lymphocytes can be compared with our findings in murine cells, in which a decrease in levels and molecular sizes of the TMC6 and TMC8 proteins were observed in thymocytes of the *Tmc6*$^{\Delta/\Delta}$ or *Tmc8*$^{\Delta/\Delta}$ mice (Fig. 1*D*). Furthermore, a decrease in CIB1 protein level was seen in *Tmc6*$^{\Delta/\Delta}$ and *Tmc8*$^{\Delta/\Delta}$ mouse thymocytes (Fig. 4*C*) and lymph node cells (Fig. 4*D*).

To understand how levels of TMC6 and TMC8 affect CIB1 levels, we first performed qRT-PCR analysis to compare the RNA levels of *Cib1*, *Tmc6*, and *Tmc8* in TMC6- and TMC8-doubly expressing Jurkat cells and control vector-transfected cells. As expected, *Tmc6* and *Tmc8* levels were substantially higher in the TMC6- and TMC8-expressing cells than in the control cells. However, *Cib1* RNA levels remained the same in those cells (Fig. 5*A*). In addition, *Cib1* RNA levels did not change in *Tmc6*$^{\Delta/\Delta}$ or *Tmc8*$^{\Delta/\Delta}$ thymocytes (Fig. S4). These results suggest that post-translational rather than transcriptional processes led to the robust elevation of CIB1 protein levels observed with TMC6 and TMC8 expression. We examined whether CIB1 levels are regulated by proteasomal degradation by treating cells with the proteasome inhibitor MG-132. Given that Jurkat cells are sensitive to apoptosis induced by proteasomal inhibitors, our analysis was limited by doses and duration of MG-132 treatment. Nevertheless, MG-132 treatment for 6–7 h elevated CIB1 levels in both parental (Fig. 5*B*) and vector-transfected Jurkat cells (Fig. 5*C*). The CIB1 level changes induced by MG-132 treatment were not detected in the TMC6/TMC8 doubly transfected cells (Fig. 5*C*), indicating that TMC6 and TMC8 expression can protect CIB1 from proteasomal degradation. We also analyzed CIB1 ubiquitination via immunoblotting of CIB1 immunoprecipitates with an anti-ubiquitin antibody. To eliminate the possibility that the detected protein ubiquitination may come from other complexed proteins, we heated the cell lysates in 1% SDS to disrupt protein interaction prior to immunoprecipitation. Indeed, polyubiquitination of CIB1 was detected in control vector-transfected cells, and CIB1 ubiquitination was elevated by MG-132 treatment. Less CIB1 polyubiquitination (in terms of the ratio relative to total protein amounts and polyubiquitin chain length) was seen in TMC6- and TMC8-expressing cells (Fig. 5*D*). These results suggest that TMC6 and TMC8 stabilize CIB1 by protecting CIB1 from ubiquitination and proteasomal degradation.

We then evaluated whether CIB1 also regulates TMC6 and TMC8 levels. We used siRNA transfection to knock down

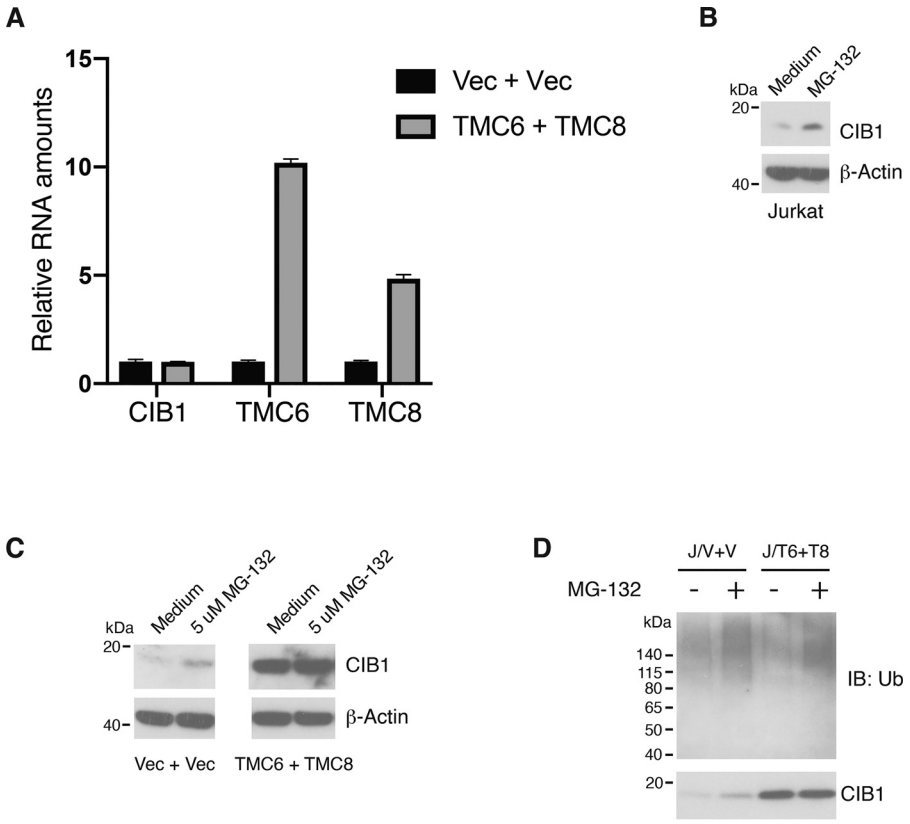

Figure 5. TMC6 and TMC8 stabilize CIB1 protein at least in part by regulating CIB1 ubiquitination and proteasomal degradation. *A*, total RNA was extracted from stable vector-transfected or FLAG-TMC6– and HA-TMC8–transfected Jurkat cells that were used in Fig. 3 and Fig. 4 and analyzed for TMC6, TMC8, and CIB1 mRNA content using real-time RT-PCR. mRNA levels are expressed relative to β-actin mRNA levels and were normalized such that expression levels in control (vector-transfected) cells = 1. *B*, parental Jurkat cells or stable vector-transfected Jurkat cells were treated with 10 μM MG-132 for 7 h. RIPA cell lysates were analyzed for CIB1 protein level using Western blotting. *C*, stable vector-transfected Jurkat cells or Jurkat cells that express FLAG-TMC6 and HA-TMC8 were treated with 5 μM MG-132 for 6 h. Cellular CIB1 protein levels were determined by immunoblotting with anti-CIB1 antibody. *D*, stable vector-transfected or FLAG-TMC6– and HA-TMC8–expressing Jurkat cells were treated with or without 20 μM MG-132 for 3 h. RIPA cell lysates that were normalized for protein content were supplemented with SDS to 1% and heated at 95 °C for 5 min to disrupt protein complexes. The heated lysates were then diluted to 0.1% SDS and immunoprecipitated with anti-CIB1 Ab. The immunoprecipitates were resolved using SDS-PAGE and immunoblotted with anti-ubiquitin or anti-CIB1 Ab.

endogenous CIB1 expression in Jurkat cells and then assayed for a change in the levels of FLAG-TMC6 and HA-TMC8 proteins. Two different CIB1 siRNAs each efficiently inhibited CIB1 expression (Fig. 6*A*). Notably, both FLAG-TMC6 and HA-TMC8 protein levels were substantially decreased in CIB1 siRNA-transfected cells, indicating that normal CIB1 expression is required for full TMC6 and TMC8 protein stability. We also assessed whether the TMC6-TMC8 interaction is mediated by CIB1 by performing a TMC6 and TMC8 co-immunoprecipitation assay after CIB1 knockdown (Fig. 6*B*). In the lysate controls (*lanes d–f*), both CIB1 siRNAs again resulted in marked decreases of CIB1 and both TMC6 and TMC8 protein levels. In the anti-FLAG-TMC6 immunoprecipitations (*lanes a–c*), despite a reduction in its level, a substantial amount of HA-TMC8 still co-immunoprecipitated with FLAG-TMC6 in cells subjected to CIB1 knockdown. The ratio of TMC6 and TMC8 in the immunoprecipitation lanes did not differ from that observed in the lysate inputs in CIB1-inhibited cells. This result is consistent with the conclusion that TMC6 and TMC8 interaction does not require CIB1.

Defects in both T cells and keratinocytes have been thought to be responsible for the development of EV (10, 11). We used

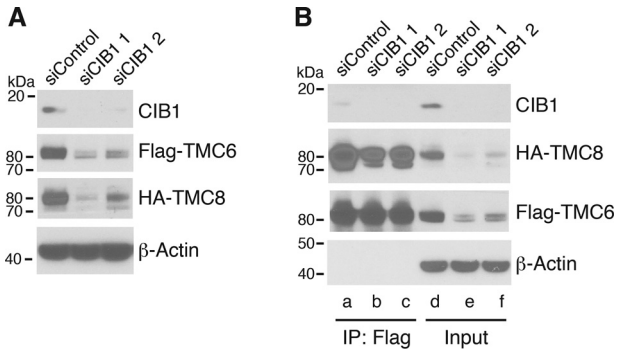

Figure 6. CIB1 stabilizes TMC6 and TMC8. Stable Jurkat cells that express FLAG-TMC6 and HA-TMC8 were transfected with control siRNA (*siControl*) or two individual CIB1 siRNAs (*siCIB1*) by electroporation. At 72 h after transfection, the cells were harvested and lysed in Triton lysis buffer. Cell lysates were normalized for protein content and levels of CIB1, FLAG-TMC6 or HA-TMC8 levels were determined using Western blotting of lysates (*A*) or anti-FLAG immunoprecipitates (*B*). *B*, the anti-FLAG-TMC6 immunoprecipitates and lysate inputs were resolved by SDS-PAGE and probed with anti-CIB1, anti-HA, or anti-FLAG Ab.

our TMC6 and TMC8 antibodies to compare TMC6, TMC8, and CIB1 protein levels in lymphocytes and keratinocytes. We determined and compared TMC6 and TMC8 levels and CIB1

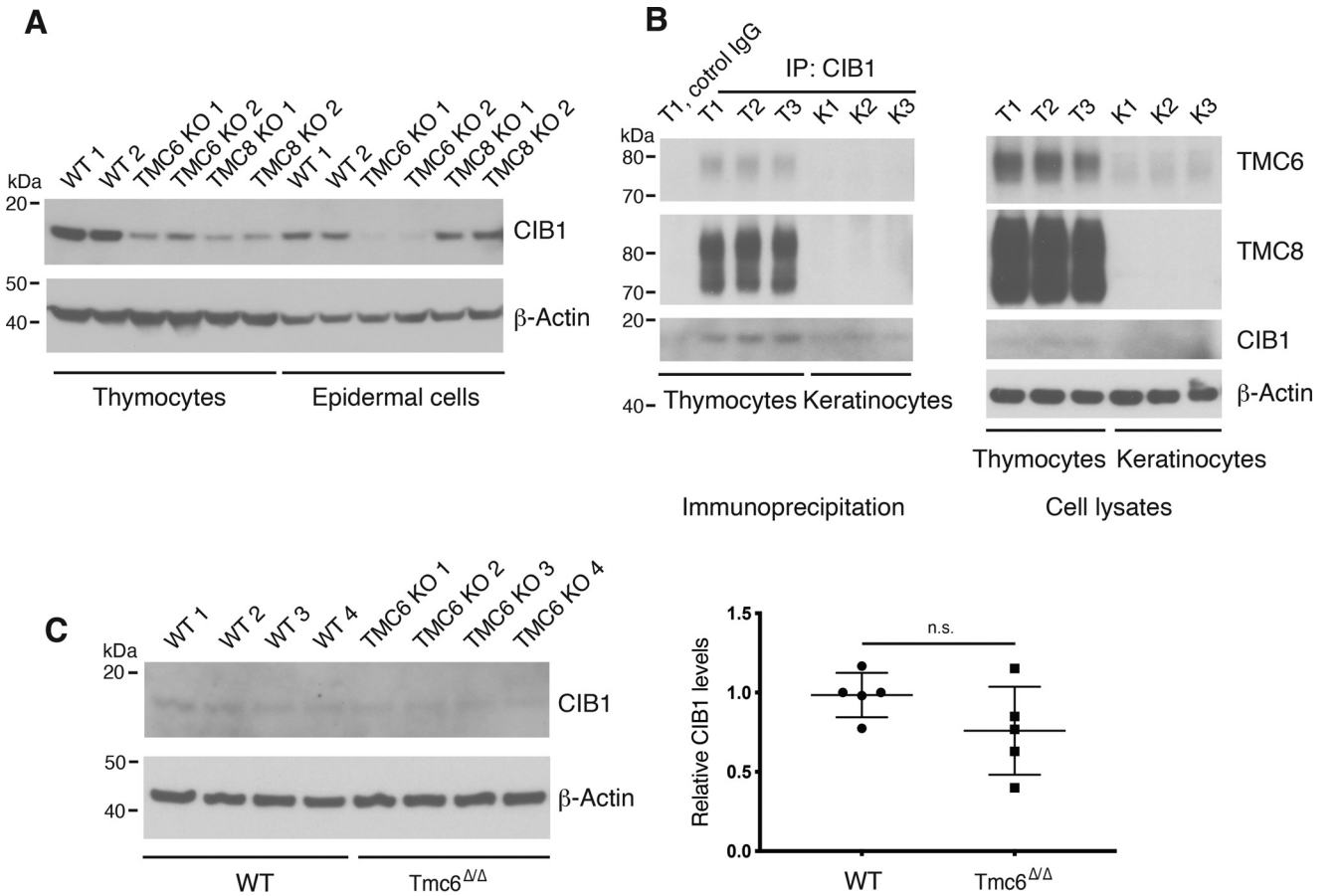

Figure 7. TMC6 and TMC8 expression levels are low and TMC6 and TMC8 are not active in regulating CIB1 levels in mouse keratinocytes. *A*, single-cell suspension of thymocytes and skin epidermal cells were prepared from the same individual 8–10-week-old female WT, *Tmc6*$^{\Delta/\Delta}$, or *Tmc8*$^{\Delta/\Delta}$ mice and lysed in RIPA buffer. Cell lysates were normalized for protein content and CIB1 levels were determined using Western blotting. *B*, keratinocytes were prepared from 3-day-old neonatal C57BL/6 mice and cultured for 24 h in low-calcium medium. Then the cultured keratinocytes and thymocytes that were freshly prepared from three 8–10-week-old C57BL/6 mice were lysed in Triton lysis buffer. Cell lysates were normalized for protein concentration and immunoprecipitated with anti-CIB1 Ab. SDS-PAGE-resolved immunoprecipitates or cell lysates were immunoblotted with anti-TMC6, anti-TMC8, or anti-CIB1. *C*, keratinocytes were prepared from four 3-day-old WT or *Tmc6*$^{\Delta/\Delta}$ mice and cultured for 24 h in low-calcium medium. Normalized cell lysates were resolved and determined for CIB1 levels using Western blotting. CIB1 band intensities in the *left panel* and another experiment were quantified and normalized to β-actin. Data are depicted as mean ± S.D. of the values relative to WT = 1. *p* value of comparison of CIB1 expression between WT (n = 5) and *Tmc6*$^{\Delta/\Delta}$ (n = 5) keratinocytes is >0.05 (*n.s.*, not significant).

levels in adult mouse epidermal cells and thymocytes. In contrast to thymocytes, TMC6 and TMC8 were not detectable in epidermal cells (Fig. S5*A*). As seen in Fig. 4*C*, CIB1 levels were dramatically down-regulated in both *Tmc6*$^{\Delta/\Delta}$ and *Tmc8*$^{\Delta/\Delta}$ thymocytes (Fig. 7*A*). However, CIB1 levels were reduced in *Tmc6*$^{\Delta/\Delta}$ epidermal cells but not in *Tmc8*$^{\Delta/\Delta}$ epidermal cells compared with WT epidermal cells (Fig. 7*A*). The possibility might exist that the failure to detect TMC6 or TMC8 in epidermal cells is caused by trypsin cleavage of the transmembrane proteins during epidermal cell suspension preparation. Some portion of lymphocytes and other types of immune cells are also present in the epidermal cell suspension (17). Therefore, we also performed a commonly adopted procedure (18) to obtain relatively pure keratinocytes and analyzed TMC6, TMC8, and CIB1 in cultured primary keratinocytes. The cells were cultured in low-calcium media that prevents keratinocyte differentiation to retain the original status of the isolated keratinocytes. TMC6 was detected in primary keratinocytes isolated from C57BL/6 mice, but the levels were 6.6-fold less than in thymocytes (Fig. 7*B* and Fig. S5*B*). A similar result was also observed for FVB mice (Fig. S5*C*). TMC8 was not detectable in cultured keratinocytes from either C57BL/6 or FVB mice (Fig. 7*B* and Fig. S5*C*). These results for mouse keratinocytes and lymphocytes are similar to those for the amounts of TMC6 and TMC8 RNA in human skin and lymphoid tissues (RRID:SCR_006710). Co-immunoprecipitation experiments showed that the TMC6-TMC8-CIB1 complex was much more easily detected in thymocytes than in keratinocytes of C57BL/6 (Fig. 7*B*) and FVB mice (Fig. S5*C*). Furthermore, compared with WT cells, little CIB1 reduction was observed in *Tmc6*$^{\Delta/\Delta}$ primary keratinocytes (Fig. 7*C*). These results demonstrate that TMC6 levels are low, TMC8 levels are lower or nonexistent, and therefore a TMC6-TMC8-CIB1 complex is not present or only present at extremely low levels in mouse keratinocytes.

Discussion

By RNA analysis and protein assays using custom-made antibodies, we observed that TMC6 and TMC8 are highly expressed in lymphocytes. TMC6 and TMC8 are frequently coexpressed in virtually all lymphoid tissues (RRID:SCR_006710).

The high expression in lymphocytes distinguishes TMC6 and TMC8 from other TMC proteins, which are usually most abundant in epithelial cells (1, 19). This coexpression pattern suggests that TMC6 and TMC8 may interact and function together.

Indeed, we observed that TMC6 and TMC8 interact and that their coexpression, compared with individual expression, induced changes in protein amounts and sizes. Homodimers were identified for the TMC-homologous protein anoctamin and recently for TMC1 (14, 20). It is not known whether TMC6 and TMC8 also form homodimers. In this study we demonstrated that TMC6 and TMC8 strongly interacted in lymphocytes and thus present the first example that TMC proteins may form heterocomplexes, which by analogy to the anoctamin structure are most likely heterodimers. Interestingly, we also observed that TMC6 and TMC8 regulate each other at the protein level in lymphocytes. Both endogenous mouse TMC6 and TMC8 and plasmid-expressed human TMC6 and TMC8 were present as doublets in lymphocytes. The largest TMC6 and TMC8 species were substantially increased in the presence of the other protein. This finding is most compatible with protein stabilization and decreased proteolysis within the heterocomplex, but addition of protein modifications or even changes because of alternative splicing cannot be ruled out. The larger TMC6 and TMC8 species appear to be more stable and may represent the fully functional forms. Heterocomplex formation could promote protein function on the cell surface and stabilize membrane proteins by preventing protein internalization (21). The findings that TMC6 and TMC8 regulate each other may help to explain that inactivating mutations in either of them might be sufficient to induce EV and that identical clinical manifestations are seen in patients with either *TMC6* or *TMC8* mutations. *TMC6* and *TMC8* genes lie in a head-to-head fashion next to each other on the same chromosome (9); however, our RNA analysis indicated that null mutation in one did not affect the transcription of the other.

Mutations of *TMC6* or *TMC8* are found in more than half of EV patients who suffer from chronic cutaneous β-HPV infections. β-HPV is prevalent, but is not virulent in healthy individuals (22). We generated TMC6 KO and TMC8 KO mice to provide an animal model to eventually study the cause of EV and the function of TMC proteins. We observed only subtle immunologic differences between KO and WT mice. We observed slightly fewer CD4 and CD8 single positive T cells in the thymus and slightly fewer CD8 T cells in lymph nodes of TMC6 KO or TMC8 KO mice[4]. It is not known whether the TMC6 or TMC8 deficiency induced modest changes in T development that might contribute to the elevated susceptibility to β-HPV infection. Experiments involving challenge with murine papillomavirus in the TMC6- or TMC8-deficient mice might help to determine the role of lymphocytes in the defense of papillomavirus infection. However, the only available mouse-tropic papillomavirus, *Mus musculus* papillomavirus type 1 (MuPV1) (23), does not belong to the β genus (16). No gross abnormalities or histological changes were observed in the skin of TMC6 KO and TMC8 KO mice.

Patients with mutant CIB1 proteins display identical clinical features to patients with TMC6 or TMC8 mutations (16). We identified a strong interaction of CIB1 with TMC6 and TMC8 and demonstrated that TMC6 and TMC8 substantially regulated CIB1 stability in T cells. CIB1 was also required for TMC6 and TMC8 stability in T cells. The molecular interactions of these three proteins likely explain the similar disease presentations of patients carrying *TMC6*, *TMC8*, or *CIB1* mutations. It appears that the TMC6-TMC8-CIB1 trimeric complex is important for mutual regulation of each protein's stability and function, either alone or as a complex. Interestingly, Tang *et al.* (24) recently reported that TMC1 and TMC2 form a complex with CIB2 and CIB3 and that CIB2/3 promotes the stability of TMC1/2. This study also revealed that the mechanosensory function of TMC1/2 in *Caenorhabditis elegans* neurons depends on CIB2/3 and their interacting protein ankyrin. CIB1 interacts with and may be regulated by many proteins including PAK1, and its pleiotropic functions have been reported (25). We detected robust co-immunoprecipitation of TMC6 and TMC8 but no co-immunoprecipitation of PAK1 (data not shown) with CIB1 in mouse thymocytes. It appears that TMC6 and TMC8 regulate CIB1 in lymphocytes because coexpression of TMC6 and TMC8 markedly elevated CIB1 levels whereas either TMC6 or TMC8 deficiency reduced CIB1 protein levels. We demonstrated that this regulation is at the protein but not the transcriptional level and that the protein complex formation is important for cellular CIB1 stabilization. Interestingly, it has been demonstrated that the CIB1 homolog CIB2 interacts with TMC1 and TMC2 in inner ear hair cells and that *CIB2* mutations lead to hearing impairment, as do mutations of *TMC1* (26, 27). Knockout of *Tmc1* or *Cib2* in mice replicates the deafness phenotype in human patients (4, 28). In the auditory system, *Tmc1* can compensate for the loss of *Tmc2* function, but not vice versa (4).

Compared with expression in lymphocytes, we found dramatically lower TMC6 protein levels and undetectable TMC8 expression in keratinocytes. TMC6 and TMC8 regulation of CIB1 in keratinocytes was limited. An extremely low TMC8 RNA level in mouse skin was also observed by others (29). Because of the lack of specific antibodies, we have not analyzed the TMC6/8 complex in human keratinocytes. However, RNA data suggest that TMC6, and especially TMC8, are also expressed at far lower levels in skin than in lymphoid tissues in humans (RRID:SCR_006710). It was reported that a putative TMC6-TMC8-CIB1 complex interacts with α-HPV E5 protein in keratinocytes, and it was postulated that the TMC6 and TMC8 mutation-promoted EV is caused by a keratinocyte-intrinsic immunity defect (16). Our study suggests that lymphocytes may be major host cells where TMC6, TMC8, and CIB1 interact and thus where TMC6 and TMC8 function is required to prevent the development of EV. Although TMC6 and TMC8 closely regulate CIB1 and CIB1 has a broad range of functions, the reported CIB1 deficiency–induced phenotypes

[4] Wu, Sommers, and Samelson, unpublished data.

did not occur in TMC6 or TMC8 KO mice or in *TMC6* or *TMC8* mutant patients. For instance, CIB1 has been linked with male fertility (30). Both TMC6 KO and TMC8 KO mice were normal in breeding. A possible explanation is that TMC6 and TMC8 are highly expressed and regulate CIB1 in specific types of tissues such as lymphoid tissues. Therefore, TMC6 and TMC8 may function through CIB1 to regulate lymphocytes. The connection of CIB1 with TMC6 and TMC8 may help the identification of TMC6 and TMC8 functions in lymphocytes.

Apart from *TMC6*, *TMC8*, and *CIB1*, biallelic mutations in a panel of other genes including *RhoH*, *STK4*, *Coro1A*, *TPP2*, *DCL RE1C*, *LCK*, *RAS GRP1*, and *DOCK8* have also been associated with EV. In contrast to *TMC6*, *TMC8*, and *CIB1* mutations, which appear to specifically promote susceptibility to some types of β-HPV infection, the patients carrying those gene mutations have variable levels of systemic T cell defects and are also prone to a range of other pathogen infections (11). Studies of animal models also demonstrated important roles of those proteins in regulating mouse T cells (31–33). In addition, EV has been reported in patients subjected to immunosuppressant treatment (34). Thus, T cell defects may contribute to the susceptibility to β-HPV infection. On the other hand, EV is not always (even rarely) seen in patients having T cell defects. There may be a multifactorial explanation for β-HPV susceptibility, or defects in some, as yet undefined, specific aspect of T cell function might be responsible. No major defect in T cells from TMC6- or TMC8-deficient patients has been discovered (16, 35, 36). However, our study underlines the necessity to further investigate the roles of TMC6 and TMC8 in lymphocytes, and in particular T cells, in addition to the recent focus on keratinocytes (16). The identification of a defect in TMC6- or TMC8-deficent T cells may provide insights into what specific T cell function is critical for combating β-HPV infection.

Experimental procedures

Animals

C57BL/6J mice were originally purchased from The Jackson Laboratory and 129S6 mice were from Taconic. FVB mice were originally purchased from Taconic. All animal breeding and procedures was performed under a protocol approved by the joint NINDS/NIDCD Animal Care and Use Committee and two protocols approved by the National Cancer Institute Animal Care and Use Committee.

RNA isolation

The brain, thymus, heart, lung, spleen, pancreas, kidney, small intestine, and epididymis were harvested from neonatal (P1) and adult (12-week) C57BL/6 mice and immediately submerged in RNAlater (Ambion). RNA was prepared using RNeasy Mini (Qiagen) and poly(A)$^+$ mRNA purification with Oligotex mRNA Mini kit (Qiagen).

RT-PCR and sequencing of Tmc6 and Tmc8 isoforms

We performed RT-PCR to verify the alternative spliced transcripts in mouse thymus and spleen SMART First-Strand cDNA by using LA-Taq DNA polymerase (Takara Bio). The primers were chosen within the sequences of 5′ and 3′ ends determined by rapid amplification of cDNA ends. PCR products were cloned into pGEM T-easy vector for sequencing.

Cell lines

Jurkat E6.1 T cells (Jurkat cells) were cultured in RPMI supplemented with 10% FBS, 100 units/ml penicillin, and 100 mg/ml streptomycin (37).

Antibodies

Anti-TMC6 and anti-TMC8 antibodies were raised in rabbits by immunization with fusion proteins composed of C-terminal mouse TMC6 or TMC8 domains fused in-frame with GST. Polyclonal anti-TMC6 Ab was used after affinity purification. Monoclonal anti-TMC8 was produced and purified from cells transfected with plasmid expressing the Ab-encoding cDNA (Abcam). Mouse monoclonal anti-CIB1, anti-FLAG, and anti-β-actin Ab were from Sigma-Aldrich, and sheep polyclonal anti-CIB1 Ab was from R&D Systems. Rat anti-HA Ab was from Roche. Anti-ubiquitin (P4D1) mAb were purchased from Santa Cruz Biotechnology.

Construction of TMC expression plasmids

PCR-amplified hTMC6 with FLAG tag at the C terminus was cloned into pMSCVpuro (BD Biosciences) at the Bgl II and EcoR I sites. PCR-amplified hTMC8 with HA tag at the C terminus was cloned into pMSCVHyg (BD Biosciences) at the Bgl II and Xho I sites. The resulting plasmids were verified by restriction enzyme digestion and DNA sequencing.

Generation of Tmc6- and Tmc8-targeting constructs

The gene-targeting construct was generated to disrupt *Tmc6* by homologous recombination. Using a genomic DNA fragment spanning 15 kb of the *Tmc6* locus obtained from a 129 × 1/SvJ mouse genomic library (Strategene), we replaced a 1.6-kb fragment containing exons 6–8 of *Tmc6* with a nuclear localization signal and *LacZ* reporter gene, which would be transcriptionally regulated by the endogenous *Tmc6* promoter through a gene trap sequence, the Engrailed-2 intron and splice acceptor site (En-2/SA), and the internal ribosome entry site (38), followed by a phosphoglycerine kinase (PGK)-neomycin resistance gene sandwiched with LoxP fragments for positive selection. A 4.8-kb fragment upstream to exon 6 flanked as 5′-arm, and a 4.6-kb fragment downstream to exon 8 as 3′-arm. The whole insert was embedded in a pPNT vector backbone with Ganciclovir herpes simplex virus-thymidine kinase cassette for negative selection. The final targeting construct was verified by restriction mapping and sequencing of the full-length insert.

Tmc8-targeting construct was generated with the same strategy described above by using a pPNT vector and a 13-kb genomic DNA fragment spanning exons 6–9 of *Tmc8* and upstream flanking sequences from a 129 × 1/SvJ mouse genomic library (Strategene) and a 9-kb genomic DNA clone encoding *Tmc8* exons 6–9 and downstream flanking sequence

from a 129/SvM mouse bacterial artificial chromosome (BAC) genomic library (Invitrogen). A 3.2-kb genomic DNA fragment containing exons 6–9 of *Tmc8* was replaced by the targeting insert, flanked by a 6-kb fragment upstream to exon 6 as the 5′-arm, and a 4-kb downstream to exon 9 as the 3′-arm.

Generation of $Tmc6^{\Delta/\Delta}$ and $Tmc8^{\Delta/\Delta}$ mice

The gene-targeting constructs were transfected into 129S6 embryonic stem (ES) cells through electroporation (Gene Pulser II, Bio-Rad) to achieve homologous recombination (39), which was verified by PCR and Southern blotting screening. Three selected clones were injected into the C57BL/6 blastocysts for chimeric mice generation. The male chimeras were backcrossed to C57BL/6 female mice, and the offspring from ES cell germ line transmission were recognized by coat color and genotyped by PCR to identify the mutant *Tmc6* allele carriers. The heterozygous mice ($Tmc6^{+/\Delta}$) were backcrossed to a germline Cre line in C57BL/6 (Jackson Laboratory) to remove the LoxP-flanked PGK-neomycin–resistant gene cassette. The homozygous *Tmc6*-disrupted mice ($Tmc6^{\Delta/\Delta}$) were generated by intercross of $Tmc6^{+/\Delta}$ offspring after five generations of backcrossing to C57BL/6 to minimize the 129S6 genetic background (<5%). $Tmc8^{\Delta/\Delta}$ mice were generated by the same procedures.

Southern blotting analysis of $Tmc6^{\Delta/\Delta}$ and $Tmc8^{\Delta/\Delta}$ mice

For Southern blotting analysis to screen the transfected ES cells or genotype the *Tmc6* and *Tmc8* gene–disrupted mice, genomic DNA was prepared from ES cell pellets or mouse liver. After overnight restriction endonuclease digestion, 10 μg of each DNA sample was fractionated on a 0.6% agarose gel and transferred to TurboBlotter Nytran nylon membrane (Whatman), followed by overnight hybridization with a P^{32}-labeled *Tmc6* (537 bp) or *Tmc8* probe (530 bp) at 42 °C. After washing, the membrane was exposed to X-ray film or scanned with a Typhoon™ Variable Mode Imager (GE Healthcare Bio-Sciences Corp.).

Northern blotting analysis of $Tmc6^{\Delta/\Delta}$ and $Tmc8^{\Delta/\Delta}$ mice

Total RNA (10 μg each) was isolated from neonatal and adult mouse tissues, denatured, fractionated on a 1% agarose gel with MOPS-formaldehyde buffer, then transferred and cross-linked to a TurboBlotter Nytran membrane. Hybridization probes were labeled using DECAprime™ II Random Priming DNA Labeling Kit (Ambion) with ^{32}P-dCTP (Perkin-Elmer), according to the manufacturer's instructions. *Tmc6* probe 1 spanned exons 5–7 (440 bp) and probe 2 spanned exons 10–15 (516 bp). *Tmc8* probe 1 spanned exons 4–8 (514 bp) and probe 2 spanned exons 12–16 (617 bp). After hybridization with a specific probe at 42 °C overnight, the membranes were visualized with a Typhoon™ Variable Mode Imager.

Cell transfection, virus infection, and derivation of stable cell lines

pMSCV plasmids containing FLAG-TMC6, HA-TMC8, and empty vectors were transfected into Jurkat cells via electroporation at 250 V for 20 s using Gene Pulser Xcell (Bio-Rad). Alternatively, the TMC6 or TMC8 pMSCV plasmids were transfected into Phoenix-Ampho cells (from Dr. Gary Nolan, Stanford University) using Lipofectamine 2000 (Thermo Fisher Scientific) to produce virus. Retrovirus-containing supernatants were collected and used to infect Jurkat cells. For deriving stable cell lines, the cells that were transduced and/or transfected with pMSCV-TMC6/8 plasmids or empty vectors were selected with 1 μg/ml puromycin or 400 μg/ml hygromycin for 10–14 days. Stable TMC transductants or transfectants were cloned via limited dilution and analyzed for TMC6 and TMC8 expression by immunoblotting.

Knockdown of protein expression by siRNA

Jurkat cells that stably express FLAG-TMC6 and HA-TMC8 were transfected with CIB1 siRNA (from MilliporeSigma) or negative control siRNA (from Thermo Fisher Scientific) with electroporation (Gene Pulser Xcell, Bio-Rad) at 250 V for 20 s. Transfected cells were harvested at 72 h after transfection and analyzed for protein levels via Western blotting.

Preparation of suspensions of lymphocytes and epidermal cells

Mouse thymus, lymph node, and spleen cells were prepared as previously described (40). Mouse epidermal cell suspensions were prepared as described by Kobayashi *et al.* (17) with a slight modification. Briefly, shaved trunk skin was removed from subcutaneous tissues using forceps, floated with the epidermal side up, and incubated with 10 ml of 0.15% trypsin and 0.27 mM EDTA at 37 °C for 40 min. The epidermis and dermis were separated manually using forceps. Epidermal cells were pipetted with force and suspended in 5% FCS in PBS, washed, and filtered through a 100-μm cell strainer (BD Biosciences).

Preparation and culturing of mouse keratinocytes

Primary keratinocytes were isolated from 2–3-day-old C57BL/6 or FVB mouse epidermis following the protocol by Lichti *et al.* (18) and cultured in calcium-free Eagle's medium supplemented with 8% Chelex-treated FCS (Gemini Bio-Products) and 0.05 mmol/liter calcium.

Quantitative RT-PCR

Total RNA was prepared using RNeasy kit (Qiagen) and reverse-transcribed with iScript cDNA synthesis kit (Bio-Rad). Quantitative RT-PCR was performed using the following primers: hTMC6 (Fwd, 5′-TGTACTACGGCCACTACAGTAA-3′; Rev, 5′-CAGGGTGATGCAGGTGATAAA-3′), hTMC8 (Fwd, 5′-CCAAGTACTCACAGGACAACAA-3′; Rev, 5′-CAGCTGGACCAGAAATGTGA-3′), hCIB1 (Fwd, 5′-CCTTGAACAGAGAAGACCTGAG-3′; Rev: 5′-CTGGAACTCAGAGAGGTTGATG-3′), hb-actin (Fwd, 5′-TTGCCGACAGGATGCAGAA-3′; Rev, 5′-GCCGATCCACACGGAGTACTT-3′), mCIB1 (Fwd, 5′-ACCCCAGACATCAAGTCACAC-3′; Rev, 5′-TCCCGTGAGGCAATTCACAAG-3′), mTMC6 (Fwd, 5′-CGTGGCCTATGCTCTGAA-3′; Rev, 5′-CTGCTGGGTCAGGTGG-

ASBMB

AAAG-3′), mTMC8 (Fwd, 5′-TTCTACGGTGCCTACC-GAG-3′; Rev, 5′-AGACCATCGGGCTAAGGAGG-3′), mb-actin (Fwd, 5′-GGCTGTATTCCCCTCCATCG-3′; Rev, 5′-CCAGTTGGTAACAATGCCATGT-3′). PCR products were generated and quantified using PowerSYBR Green PCR Master Mix (Applied Biosystems, University Park, IL) on an Applied Biosystem real-time PCR instrument (QuantStuidio 5). b-Actin was used for normalization, immunoblotting, immunoprecipitation, and co-immunoprecipitation.

The cells were lysed with Triton X-100 lysis buffer or RIPA lysis buffer as indicated and normalized for protein content using a Bradford protein assay (Bio-Rad) (21). TMC6, TMC8, and CIB1 levels were assessed by immunoblotting with antibodies against those proteins. To detect and quantify CIB1 ubiquitination, the cells were lysed in RIPA buffer. The resulting cell lysates were normalized for protein concentration, SDS was added to 1% concentration, and lysates were heated at 95 °C for 5 min then diluted to SDS at 0.1% and immunoprecipitated with anti-CIB1 prior to blotting with anti-ubiquitin Ab. Protein associations were assessed via co-immunoprecipitation of proteins from Triton X-100 lysates as previously described (21). For Western blotting, proteins in immunoprecipitates or cell lysates were resolved by SDS-PAGE and transferred onto nitrocellulose membranes that were subsequently incubated with the indicated Ab. Proteins of interest were visualized using HRP-conjugated secondary Ab (Jackson ImmunoResearch Laboratories) and enhanced chemiluminescence (Thermo Fisher Scientific). Intensities of protein bands were quantified using densitometry and ImageJ software (NIH).

Identification of TMC6- and TMC8-associated proteins via MS

FLAG-TMC6– and HA-TMC8–expressing Jurkat cells or control cells were lysed in Triton X-100 lysis buffer and the cell lysates were incubated with anti-FLAG or anti-HA antibody followed by incubation with Protein G-Sepharose 4B beads. The immunoprecipitates on beads were digested with trypsin and the resulting peptide mixture was subjected to nanoflow liquid chromatography (Thermo Easy nLC 1000, Thermo Fisher Scientific) coupled to high-resolution tandem MS (QE-HF, Thermo Fisher Scientific). MS scans were performed in the Orbitrap analyzer at a resolution of 60,000 with an ion accumulation target set at $3e^6$ over a mass range of 380–1580 m/z, followed by MS/MS analysis with an ion accumulation target set at $2e^5$ at a resolution of 15,000. Acquired MS/MS spectra were searched against a human Uniprot protein database using a SEQUEST, and the resulting peptides were filtered using the percolator validator algorithms in the Proteome Discoverer 2.2 software (Thermo Fisher Scientific).

Identification of TMC6-TMC8-CIB1 trimers

Jurkat cells that stably express FLAG-TMC6 and HA-TMC8 were treated with 2 mM of the membrane-permeable and cleavable cross-linker DSP (Thermo Fisher Scientific) or vehicle DMSO in PBS at room temperature for 30 min and then quenched in 50 mM glycine in PBS for another 10 min. Triton X-100 cell lysates were resolved on NuPAGE 4–12% Bis-Tris gel (Thermo Fisher Scientific) under nonreducing conditions and immunoblotted with anti-CIB1 antibody to detect CIB1 complexes. In parallel lanes, the CIB1 complex bands in the DSP lane or the corresponding slices of the same molecular size in the DMSO-treated control lane were excised, homogenized, and eluted in reducing sample buffer. The elutes were resolved on another SDS-PAGE and immunoblotted with specific antibodies to determine the presence of the individual proteins in the CIB1 complexes.

Lymphocyte purification and flow cytometry

Thymus, lymph node, and splenic lymphocytes were prepared and stained as previously described (40). Lymphocytes from lymph nodes and spleen were purified for CD4 or CD8 T cells or B cells via negative selection using Easysep kits (STEMCELL Technologies, Vancouver, Canada) following the manufacturer's instructions. Flow cytometry data were acquired on FACSCalibur or LSR Fortessa cytometers (BD Biosciences) and analyzed with FlowJo (TreeStar) software.

Statistics

Probability values were calculated using the Student's t test or one-way analysis of variance.

Data availability

All data are contained within this article and in the supporting information.

Acknowledgments—We thank Thorkell Andresson and Sudipto Das (Protein Characterization Laboratory, Frederick National Laboratory for Cancer Research) for mass spectrometry analysis, Eric Wawrousek (Genetic Engineering Core, National Eye Institute) for microinjecting blastocysts, Luowei Li and Stuart Yuspa (Center for Cancer Research, National Cancer Institute) for providing low-calcium medium for keratinocyte culturing, Terri Stull for animal husbandry, and Ana Dios-Esponera and Melanie Vacchio for helpful discussion.

Author contributions—C.-J. W., C. L. S., K. K., A. J. G., and L. E. S. conceptualization; C.-J. W., X. L., C. L. S., K. K., S. H., G. B., L. D., W. L., A. J. G., and L. E. S. data curation; C.-J. W., X. L., C. L. S., K. K., S. H., G. B., L. D., A. J. G., and L. E. S. formal analysis; C.-J. W. and K. K. validation; C.-J. W., X. L., C. L. S., K. K., S. H., G. B., L. D., W. L., and A. J. G. investigation; C.-J. W. and K. K. visualization; C.-J. W., X. L., C. L. S., K. K., S. H., G. B., L. D., and W. L. methodology; C.-J. W. and K. K. writing-original draft; C. L. S., A. J. G., and L. E. S. resources; C. L. S., G. B., A. J. G., and L. E. S. supervision; C. L. S., A. J. G., and L. E. S. funding acquisition; C. L. S., A. J. G., and L. E. S. project administration; C. L. S., A. J. G., and L. E. S. writing-review and editing.

Funding and additional information—This work was supported by the Intramural Research Programs of the NCI, NIDCD, and NEI, National Institutes of Health. The content is solely the responsibility of the authors and does not necessarily represent the official views of the National Institutes of Health.

Conflict of interest—The authors declare that they have no conflicts of interest with the contents of this article.

Abbreviations—The abbreviations used are: TMC, transmembrane channel-like; CIB1, calcium and integrin-binding protein 1; HPV, human papillomavirus; EV, epidermodysplasia verruciformis; PSM, peptide spectrum match; DSP, dithiobis(succinimidyl propionate); ES, embryonic stem.

References

1. Kurima, K., Yang, Y., Sorber, K., and Griffith, A. J. (2003) Characterization of the transmembrane channel-like (TMC) gene family: functional clues from hearing loss and epidermodysplasia verruciformis. *Genomics* **82,** 300–308 CrossRef Medline
2. Labay, V., Weichert, R. M., Makishima, T., and Griffith, A. J. (2010) Topology of transmembrane channel-like gene 1 protein. *Biochemistry* **49,** 8592–8598 CrossRef Medline
3. Kawashima, Y., Kurima, K., Pan, B., Griffith, A. J., and Holt, J. R. (2015) Transmembrane channel-like (TMC) genes are required for auditory and vestibular mechanosensation. *Pflügers Arch.* **467,** 85–94 CrossRef Medline
4. Kawashima, Y., Géléoc, G. S., Kurima, K., Labay, V., Lelli, A., Asai, Y., Makishima, T., Wu, D. K., Della Santina, C. C., Holt, J. R., and Griffith, A. J. (2011) Mechanotransduction in mouse inner ear hair cells requires transmembrane channel-like genes. *J. Clin. Invest.* **121,** 4796–4809 CrossRef Medline
5. Pan, B., Géléoc, G. S., Asai, Y., Horwitz, G. C., Kurima, K., Ishikawa, K., Kawashima, Y., Griffith, A. J., and Holt, J. R. (2013) TMC1 and TMC2 are components of the mechanotransduction channel in hair cells of the mammalian inner ear. *Neuron* **79,** 504–515 CrossRef Medline
6. Kurima, K., Ebrahim, S., Pan, B., Sedlacek, M., Sengupta, P., Millis, B. A., Cui, R., Nakanishi, H., Fujikawa, T., Kawashima, Y., Choi, B. Y., Monahan, K., Holt, J. R., Griffith, A. J., and Kachar, B. (2015) TMC1 and TMC2 localize at the site of mechanotransduction in mammalian inner ear hair cell stereocilia. *Cell Rep.* **12,** 1606–1617 CrossRef Medline
7. Pan, B., Akyuz, N., Liu, X. P., Asai, Y., Nist-Lund, C., Kurima, K., Derfler, B. H., Gyorgy, B., Limapichat, W., Walujkar, S., Wimalasena, L. N., Sotomayor, M., Corey, D. P., and Holt, J. R. (2018) TMC1 forms the pore of mechanosensory transduction channels in vertebrate inner ear hair cells. *Neuron* **99,** 736–753.e6 CrossRef Medline
8. Jia, Y., Zhao, Y., Kusakizako, T., Wang, Y., Pan, C., Zhang, Y., Nureki, O., Hattori, M., and Yan, Z. (2020) TMC1 and TMC2 proteins are pore-forming subunits of mechanosensitive ion channels. *Neuron* **105,** 310–321.e3 CrossRef Medline
9. Ramoz, N., Rueda, L. A., Bouadjar, B., Montoya, L. S., Orth, G., and Favre, M. (2002) Mutations in two adjacent novel genes are associated with epidermodysplasia verruciformis. *Nat. Genet.* **32,** 579–581 CrossRef Medline
10. Ovits, C. G., Amin, B. D., and Halverstam, C. (2017) Acquired epidermodysplasia verruciformis and its relationship to immunosuppressive therapy: report of a case and review of the literature. *J. Drugs Dermatol.* **16,** 701–704 Medline
11. de Jong, S. J., Imahorn, E., Itin, P., Uitto, J., Orth, G., Jouanguy, E., Casanova, J. L., and Burger, B. (2018) Epidermodysplasia verruciformis: inborn errors of immunity to human β-papillomaviruses. *Front. Microbiol.* **9,** 1222 CrossRef Medline
12. Whitlock, J. M., and Hartzell, H. C. (2017) Anoctamins/TMEM16 proteins: chloride channels flirting with lipids and extracellular vesicles. *Annu. Rev. Physiol.* **79,** 119–143 CrossRef Medline
13. Fallah, G., Römer, T., Detro-Dassen, S., Braam, U., Markwardt, F., and Schmalzing, G. (2011) TMEM16A(a)/anoctamin-1 shares a homodimeric architecture with CLC chloride channels. *Mol. Cell. Proteomics* **10,** M110.004697 CrossRef Medline
14. Brunner, J. D., Lim, N. K., Schenck, S., Duerst, A., and Dutzler, R. (2014) X-ray structure of a calcium-activated TMEM16 lipid scramblase. *Nature* **516,** 207–212 CrossRef Medline
15. Hahn, Y., Kim, D. S., Pastan, I. H., and Lee, B. (2009) Anoctamin and transmembrane channel-like proteins are evolutionarily related. *Int. J. Mol. Med.* **24,** 51–55 CrossRef Medline
16. de Jong, S. J., Créquer, A., Matos, I., Hum, D., Gunasekharan, V., Lorenzo, L., Jabot-Hanin, F., Imahorn, E., Arias, A. A., Vahidnezhad, H., Youssefian, L., Markle, J. G., Patin, E., D'Amico, A., Wang, C. Q. F., *et al.* (2018) The human CIB1-EVER1-EVER2 complex governs keratinocyte-intrinsic immunity to β-papillomaviruses. *J. Exp. Med.* **215,** 2289–2310 CrossRef Medline
17. Kobayashi, T., Glatz, M., Horiuchi, K., Kawasaki, H., Akiyama, H., Kaplan, D. H., Kong, H. H., Amagai, M., and Nagao, K. (2015) Dysbiosis and *Staphylococcus aureus* colonization drives inflammation in atopic dermatitis. *Immunity* **42,** 756–766 CrossRef Medline
18. Lichti, U., Anders, J., and Yuspa, S. H. (2008) Isolation and short-term culture of primary keratinocytes, hair follicle populations and dermal cells from newborn mice and keratinocytes from adult mice for in vitro analysis and for grafting to immunodeficient mice. *Nat. Protoc.* **3,** 799–810 CrossRef Medline
19. Keresztes, G., Mutai, H., and Heller, S. (2003) TMC and EVER genes belong to a larger novel family, the TMC gene family encoding transmembrane proteins. *BMC Genomics* **4,** 24 CrossRef Medline
20. Ballesteros, A., Fenollar-Ferrer, C., and Swartz, K. J. (2018) Structural relationship between the putative hair cell mechanotransduction channel TMC1 and TMEM16 proteins. *eLife* **7,** e38433 CrossRef Medline
21. Wu, C. J., Feng, X., Lu, M., Morimura, S., and Udey, M. C. (2017) Matriptase-mediated cleavage of EpCAM destabilizes claudins and dysregulates intestinal epithelial homeostasis. *J. Clin. Invest.* **127,** 623–634 CrossRef Medline
22. Tommasino, M. (2017) The biology of β human papillomaviruses. *Virus Res.* **231,** 128–138 CrossRef Medline
23. Ingle, A., Ghim, S., Joh, J., Chepkoech, I., Bennett Jenson, A., and Sundberg, J. P. (2011) Novel laboratory mouse papillomavirus (MusPV) infection. *Vet. Pathol.* **48,** 500–505 CrossRef Medline
24. Tang, Y. Q., Lee, S. A., Rahman, M., Vanapalli, S. A., Lu, H., and Schafer, W. R. (2020) Ankyrin is an intracellular tether for TMC mechanotransduction channels. *Neuron* **107,** 112–125.e10 CrossRef Medline
25. Leisner, T. M., Freeman, T. C., Black, J. L., and Parise, L. V. (2016) CIB1: a small protein with big ambitions. *FASEB J.* **30,** 2640–2650 CrossRef Medline
26. Giese, A. P. J., Tang, Y. Q., Sinha, G. P., Bowl, M. R., Goldring, A. C., Parker, A., Freeman, M. J., Brown, S. D. M., Riazuddin, S., Fettiplace, R., Schafer, W. R., Frolenkov, G. I., and Ahmed, Z. M. (2017) CIB2 interacts with TMC1 and TMC2 and is essential for mechanotransduction in auditory hair cells. *Nat. Commun.* **8,** 43 CrossRef Medline
27. Riazuddin, S., Belyantseva, I. A., Giese, A. P., Lee, K., Indzhykulian, A. A., Nandamuri, S. P., Yousaf, R., Sinha, G. P., Lee, S., Terrell, D., Hegde, R. S., Ali, R. A., Anwar, S., Andrade-Elizondo, P. B., Sirmaci, A., *et al.* (2012) Alterations of the CIB2 calcium- and integrin-binding protein cause Usher syndrome type 1J and nonsyndromic deafness DFNB48. *Nat. Genet.* **44,** 1265–1271 CrossRef Medline
28. Wang, Y., Li, J., Yao, X., Li, W., Du, H., Tang, M., Xiong, W., Chai, R., and Xu, Z. (2017) Loss of CIB2 causes profound hearing loss and abolishes mechanoelectrical transduction in mice. *Front. Mol. Neurosci.* **10,** 401 CrossRef Medline
29. Lazarczyk, M., Dalard, C., Hayder, M., Dupre, L., Pignolet, B., Majewski, S., Vuillier, F., Favre, M., and Liblau, R. S. (2012) EVER proteins, key elements of the natural anti-human papillomavirus barrier, are regulated upon T-cell activation. *PLoS ONE* **7,** e39995 CrossRef Medline
30. Yuan, W., Leisner, T. M., McFadden, A. W., Clark, S., Hiller, S., Maeda, N., O'Brien, D. A., and Parise, L. V. (2006) CIB1 is essential for mouse spermatogenesis. *Mol. Cell Biol.* **26,** 8507–8514 CrossRef Medline
31. Gu, Y., Chae, H. D., Siefring, J. E., Jasti, A. C., Hildeman, D. A., and Williams, D. A. (2006) RhoH GTPase recruits and activates Zap70 required for T cell receptor signaling and thymocyte development. *Nat. Immunol.* **7,** 1182–1190 CrossRef Medline
32. Du, X., Shi, H., Li, J., Dong, Y., Liang, J., Ye, J., Kong, S., Zhang, S., Zhong, T., Yuan, Z., Xu, T., Zhuang, Y., Zheng, B., Geng, J. G., and Tao, W. (2014) Mst1/Mst2 regulate development and function of regulatory T cells

through modulation of Foxo1/Foxo3 stability in autoimmune disease. *J. Immunol.* **192,** 1525–1535 CrossRef Medline

33. Janssen, E., Tohme, M., Hedayat, M., Leick, M., Kumari, S., Ramesh, N., Massaad, M. J., Ullas, S., Azcutia, V., Goodnow, C. C., Randall, K. L., Qiao, Q., Wu, H., Al-Herz, W., Cox, D., *et al.* (2016) A DOCK8-WIP-WASp complex links T cell receptors to the actin cytoskeleton. *J. Clin. Invest.* **126,** 3837–3851 CrossRef Medline
34. Zampetti, A., Giurdanella, F., Manco, S., Linder, D., Gnarra, M., Guerriero, G., and Feliciani, C. (2013) Acquired epidermodysplasia verruciformis: a comprehensive review and a proposal for treatment. *Dermatol. Surg.* **39,** 974–980 CrossRef Medline
35. Crequer, A., Troeger, A., Patin, E., Ma, C. S., Picard, C., Pedergnana, V., Fieschi, C., Lim, A., Abhyankar, A., Gineau, L., Mueller-Fleckenstein, I., Schmidt, M., Taieb, A., Krueger, J., Abel, L., *et al.* (2012) Human RHOH deficiency causes T cell defects and susceptibility to EV-HPV infections. *J. Clin. Invest.* **122,** 3239–3247 CrossRef Medline
36. Azzimonti, B., Mondini, M., De Andrea, M., Gioia, D., Dianzani, U., Mesturini, R., Leigheb, G., Tiberio, R., Landolfo, S., and Gariglio, M. (2005) CD8+ T-cell lymphocytopenia and lack of EVER mutations in a patient with clinically and virologically typical epidermodysplasia verruciformis. *Arch. Dermatol.* **141,** 1323–1325 CrossRef Medline
37. Yi, J., Balagopalan, L., Nguyen, T., McIntire, K. M., and Samelson, L. E. (2019) TCR microclusters form spatially segregated domains and sequentially assemble in calcium-dependent kinetic steps. *Nat. Commun.* **10,** 277 CrossRef Medline
38. Mountford, P. S., and Smith, A. G. (1995) Internal ribosome entry sites and dicistronic RNAs in mammalian transgenesis. *Trends Genet.* **11,** 179–184 CrossRef
39. Thomas, K. R., and Capecchi, M. R. (1987) Site-directed mutagenesis by gene targeting in mouse embryo-derived stem cells. *Cell* **51,** 503–512 CrossRef Medline
40. Sommers, C. L., Lee, J., Steiner, K. L., Gurson, J. M., Depersis, C. L., El-Khoury, D., Fuller, C. L., Shores, E. W., Love, P. E., and Samelson, L. E. (2005) Mutation of the phospholipase C-γ1-binding site of LAT affects both positive and negative thymocyte selection. *J. Exp. Med.* **201,** 1125–1134 CrossRef Medline